JOURNAL OF GEOPHYSICAL RESEARCH, VOL. 98, NO. B7, PAGES 11,935–11,940, JULY 10, 1993

Fractal and Length Analysis of Fractures During Brittle to Ductile Changes

B. VELDE,[1] D. MOORE,[2] A. BADRI,[3] AND B. LEDESERT

Linear Cantor's dust type fractal analysis of spacial distribution and fracture length analysis has been made on the fracture sets obtained in four deformation experiments performed at different confining pressures (0.5 to 5 kbar) using the Barre Granite. The fractures, mapped using petrographic microscope methods, were subsequently classed into those of shear, tension, and relaxation or decompression origin. Fracture lengths were found to have a distribution similar to a log normal frequency distribution for all sets. The difference between the mean lengths for the fractures of different orientations in a given experiment decreases with pressure, ie. the fracture lengths for all orientations (stress origins) tend to be more homogeneous as confining pressure increases. The fracture sets were also subjected to the linear Cantor's dust method of analysis. These analyses show that the fractal dimension for all of the fractures in a sample increases slightly as confining pressure increases. The difference in fractal dimension of individual fracture sets in a sample (shear, tension, decompression) tends to decrease with increased confining pressure. In the experiments with the lowest confining pressure, one finds the greatest contrasts in both fracture length and fractal dimension for fractures of different origin. These analyses show that one can describe the differences in fracture style in fracture fields using fractal measurements and length measurements. This follows the change from anisotropic stress fields to those more homogeneous through an increase of confining pressure. This shows that one can measure the change in fracture style in going from brittle rupture toward plastic deformation.

INTRODUCTION

The problem of description of geologic events and phenomena is a major one. Numerical treatment is often difficult in that geologic phenomena are complex depending upon several variables. Deformation of rocks has been performed in the laboratory for several decades but rarely has one attempted to describe, numerically, the pattern of rupture produced. The classic study of *Peng and Johnson*, [1992] has shown the types of fracture patterns produced as confining pressure is increased in a triaxial compression experiment on limestone. The triaxial deformation experiment is of course the most applicable to the greatest number of tectonic events observed by structural geologists. Figure 1 shows the basic pattern of crack distribution found in these experiments. This model has been used repeatedly in textbooks and scientific papers since its first publication (see *Goodman* [1989] or *Chernyshev and Dearman* [1991] for excellent descriptions). The salient features are the change in the dominance of primary tension cracks parallel to the major pressure compression axis, $\sigma 1$, to those due to shear forces at 45° angles to the $\sigma 1$ axis. The change in fracture pattern is accompanied by an increase in strain deformation of the sample, as indicated by the shape of the sample after the experiment. Given this rather simple schema, it will be important to describe this change in fracture style. Our aim here is to initiate a numerical description of fracture patterns using samples deformed in the laboratory.

[1]Département de Géologie, Ecole Normale Supérieure, Paris.
[2]U.S. Geological Survey, Menlo Park, California.
[3]Laboratoire de Méchanique des Fluides, Université de Poitiers, Poitiers, France.
[4]Laboratoire des Altérations Hydrothermales, Université de Poitiers, Poitiers, France.

Paper number 92JB02663.
0148-0227/93/92JB-02663$05.00

EXPERIMENTAL METHODS

Deformation

The samples have been deformed under varying conditions of confining pressure. The range reported here is from 0.5 to 5 kbar. The starting material is the Barre Granite. Experimental methods have been described in detail by *Moore et al.* [1990; 1991]. Essentially, the deformation vector ($\sigma 1$) is applied at a constant strain rate until the sample fails under compression. Loading is continued until further failure occurs along the central fault. The 0.5 and 1 kbar confining pressure samples slid stably after failure and the 3 and 5 kbar samples showed stick-slip motion. The applied axial pressure necessary to produce the first major failure increases with the confining pressure in a roughly linear manner (Figure 2).

Fracture Mapping

The deformed specimen was then cut into a petrographic thin section along the major deformation axis of the sample and perpendicular to the major fault. The sample in thin section was of slightly variable size but usually about 24x39 mm. The fractures were mapped using a petrographic microscope with transmitted light. This means that the fractures had to be visible for much of the 30 μm thickness of the thin section. Other, surface techniques might reveal a slightly different set of fracture patterns. The lower limit of resolution for this mapping method is about 0.2 mm length. These maps have been published in detail by *Moore et al.* [1991] and hence they are not given in full here. In each specimen the major failure in the cylindrical specimen produced a transversal shear zone whose orientation with respect to $\sigma 1$ changes slightly with the confining pressure [*Moore et al.*, 1990]. This brecciated zone has not been considered in the present study because the many fractures contained within it represent a major disaggregation of the rock which is not appropriate for petrographic fracture analysis. Also, the great complexity of the fractures made it impossible to map them with any degree of accuracy.

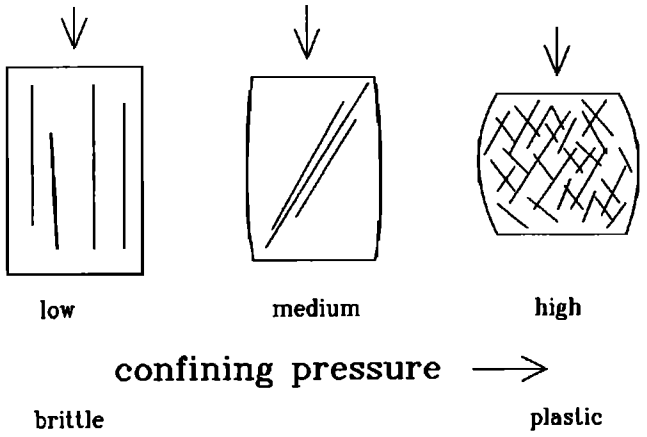

Fig.1. Schematic representation of the deformation and fracture style in carbonate rocks subjected to triaxial experiments. An increase in confining pressure in the experiment favors a plastic type of deformation.

Image Analysis

The fracture maps were subjected to image analysis using a video interface (see *Velde et al.* [1990] for details) which measured the fracture lengths and spacial distribution with a analysis of the fracture distributions was done on the fractures selected according to their orientation with respect to the $\sigma 1$ axis. Tension cracks were taken as being parallel to the $\sigma 1$ axis $\pm$ 10°, decompression fractures were taken as horizontal $\pm$ 10° and shear fractures were found to lie between 25° and 40° with ranges $\pm$ 15°. The major fault orientation changes with confining pressure from near 22 to about 40° over the pressure range studied [*Moore et al.*, 1990]. The shear fractures were classed as type 1 being parallel to the major shear fault zone, and type 2 being approximately perpendicular to it. All fractures were classed into one or the other of the above groups. These orientations are shown in Figure 3. In some cases a fracture appeared to be curved, ie. no definite linear intersection of two cracks could be determined on the mapping scale. However, scanning electron microscope work has indicated that in fact these curved cracks are composed of two or more smaller, intersecting cracks. At the scale of our investigation, the curved cracks were considered to be linear, taken as the average direction of the ensemble. A typical fracture map and the derived fracture sets is given in Figure 4.

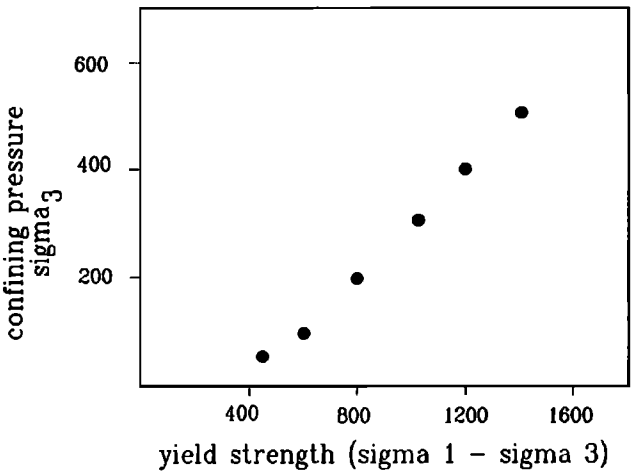

Fig.2. Relations between confining pressure and differential stress of rupture (yield strength) for the Barre granite experiments. Pressures in bars.

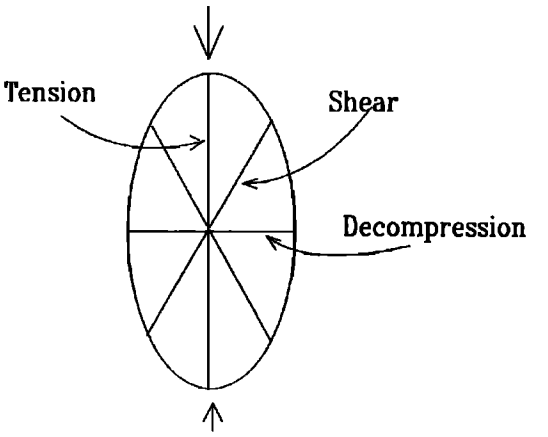

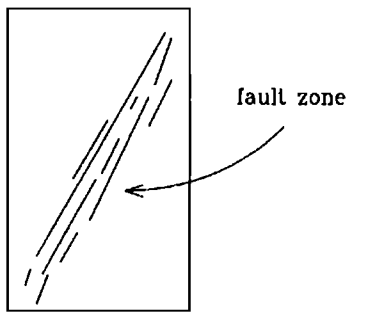

Fig.3. Representation of the different type of fractures and fracture orientations as a function of the principal stress applied to the samples in the triaxial experiments. The lower figure shows a two dimensional cut (as in the thin linear method of Cantor's dust fractal analysis). Fractal sections studied perpendicular to the $\sigma 1$ stress in the cylindrical granite sample.

EXPERIMENTAL RESULTS

Fracture Length Distributions

The fracture length frequencies in all cases form what can be only approximately described as a lognormal type of distribution. As is evident from the plots, there is a residual asymmetry toward the long fracture lengths. This can be due to two causes, either the optical method used does linear method of Cantor's dust fractal analysis. Fractal not account for all of the smaller fractures or the distribution is simply more complicated than a log normal one. This last hypothesis is apparently often the case in other examples of geological phenomena [*Rock*, 1988]. For easier visual comparison we treat the data as a normal distribution by changing the length dimension from linear to a log scale [*Rock*, 1988]. However, several authors have found that natural and experimental fracture length distributions can be

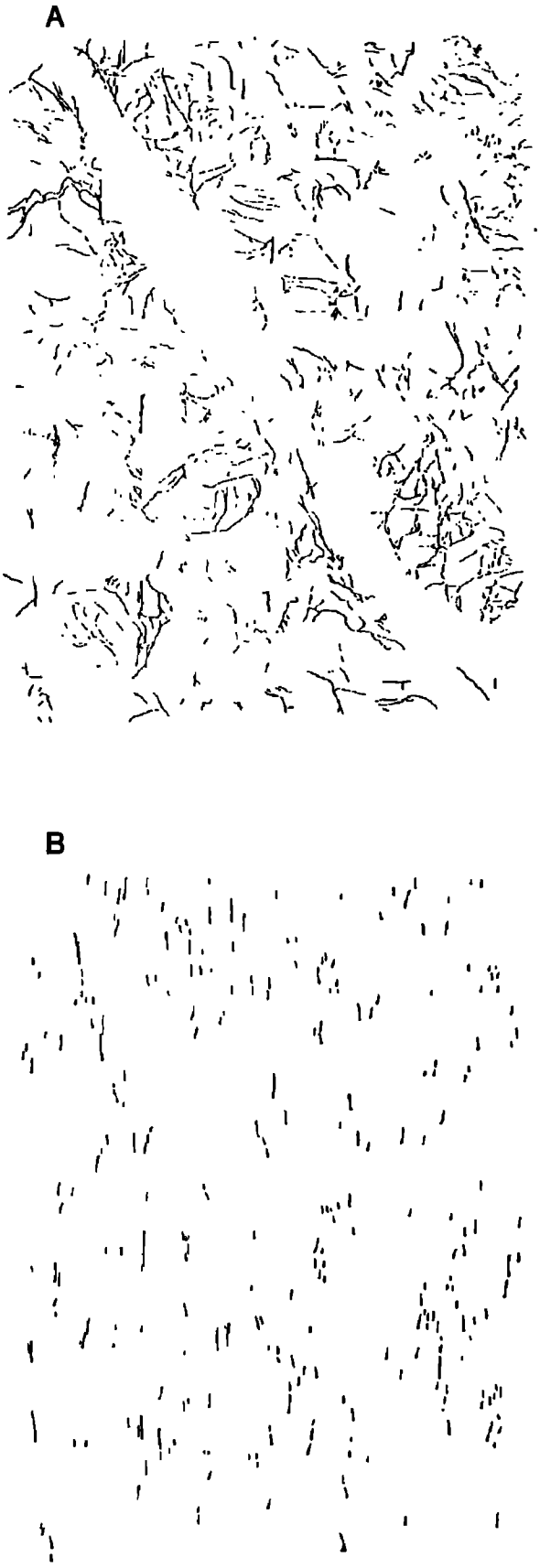

Fig.4. Example of mapped fracture sets. (a) the five kilobar confining pressure experiment and (b) the tension fracture set determined according to their parrallel orientation with respect to $\sigma 1$, vertical direction ini the figure.

TABLE 1. Fracture Lengths

	Pressure, kbar			
	0.5	1	3	5
Decompression	0.69	0.67	0.44	0.56
Tension	0.66	0.51	0.54	0.52
Shear 1	0.49	0.54	0.60	0.48
Shear 2	0.62	0.53	0.49	0.55
Difference	0.20	0.14	0.16	0.08
Total fracture length	492	520	822	591
Total fractures	689	787	1317	1018
Average fracture length	0.71	0.66	0.62	0.58

Fracture lengths are in millimeters.

assimilated to power law distribution. *Davy et al.* [1992] describe these relations in detail for data derived from two dimensional deformation experiments. In these data sets and those derived from obvservations on natural fractures on a metric scale [*Villemin et al.*, 1987; *Scholz and Cowie*, 1990; *Gudmundsson*, 1987] there appears to be no maximum in the frequency distribution, which sets this information apart from that in the present report. We do not know why this difference exists. Table 1 gives the average lengths for each orientation in millimeters. This average is slightly greater than the apparent mode values seen in the figures which are given on a log length scale. Total fracture length (in millimeters) and number of fractures are also included. The evolution of the fracture lengths as a function of confining pressure is very striking. The average lengths for the different fracture orientations show that at lowest confining pressure the difference between greatest and smallest values is 0.20 mm while at highest confining pressure the differences are only 0.08 mm. The modes, seen on the log length scale shown in Figure 5, are virtually identical at highest confining pressure. The fracture length distribution becomes very homogeneous as confining pressure is increased. Table 1 gives the total number of fractures observed in each experiment and the total lengths for the different orientations. Vertical fractures of dynamic tension origin show a decrease in average length with confining pressure as do the fractures of decompression origin. Shear fractures are more erratic in behavior. Total fractures counted show an increase then a decrease in both number and total length as confining pressure increases. At the scale of the observations the 3 kbar sample appears to be the most fractured of the samples using both criteria. It is striking to find that the total number and length of fractures decreases in the experiment of highest pressure (5 kbar). We believe that this effect is more apparent than real. As our lower limit of observation length was constant in the analysis, we cannot take into account an increase in the number of cracks which could have lengths below these limits. Since the average length of the observed cracks decreases with pressure, one could expect that there is a transfer in deformation mode to cracks of smaller sizes. The total number and length should continue to increase as more energy is absorbed by the system, but we do not see it. The normal tendency in a change from brittle (elastic) to plastic deformation will be toward smaller and smaller cracks.

Fractal Analyses

The fractal determination, made using a linear Cantor's Dust analysis as from *Velde et al.* [1990], was performed on the zones outside of the fault or shear breccia area only.

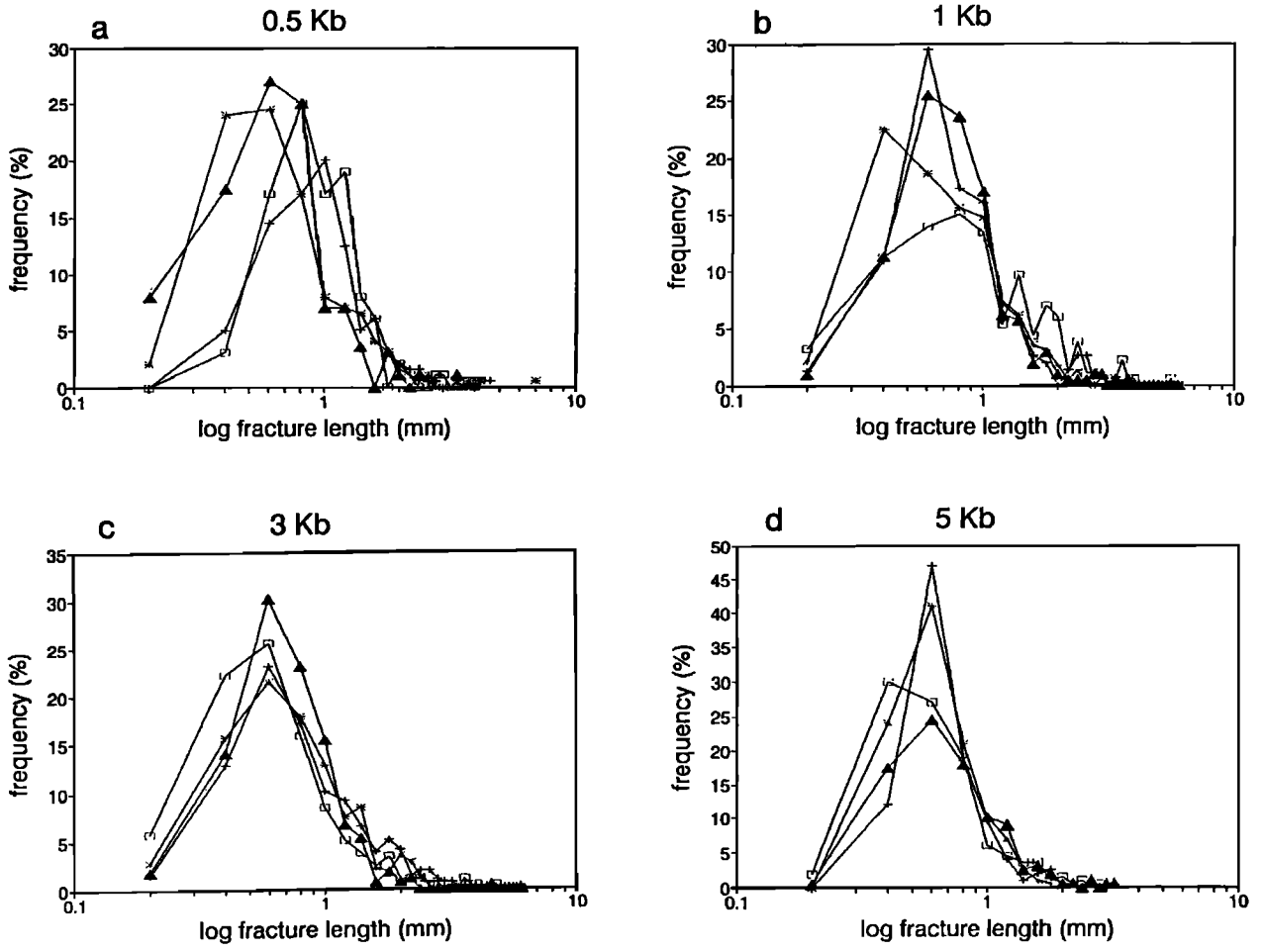

Fig.5. Frequencies (in percent) of fracture lengths (log scale) for the four various orientations (two shear directions, tension and decompression) and different confining pressures. Squares are decompression fractures (perpendicular to $\sigma 1$), stars tension (parallel to $\sigma 1$), triangles shear parallel to the fault zone, and crosses shear fractures conjugate with the central major fault zone.

The analysis lines for the Cantor's dust determination were continued from one side of the faulted zone to the other omitting the breccia zone (Figures 3 and 4) as if it did not exist. As in previous studies [*Velde et al.*, 1990; *Velde et al.*, 1991; *Merceron and Velde*, 1991], the analysis is constructed by adding one analysis line to the next in going from top to bottom of the image thus creating a continuous line of analysis which is divided into sectors of different length as the analysis proceeds. The intersection of a fracture with the analysis line is identified as a position in this linear space. The linear space is divided into segments of x length and the number of lengths containing a fault intersection is counted and compared to the total of the units in the analysis line. The analysis interval length is changed to x1 and the operation repeated. Two types of measurement interval are to be avoided. The first is where the interval is so large that all intervals in the analysis line are intersected by at least one fracture. Further augmentation of the analysis interval gives a nonsignificant result. The second is where the analysis interval is so small that only one intersection will occur in any given interval. Further division into smaller units gives a constant, meaningless relation between the number of events recorded and the total number of intervals. Useful measurement unit lengths, neither too small nor too large, were estimated from a preliminary trial in the first part of the analysis program. Ten useful measurement lengths between these limits were established on an exponentially increasing scale in order to disperse the measuement points in the graphical analysis space. A schematic representation of the measurement setup is given in Figure 6. The Can-

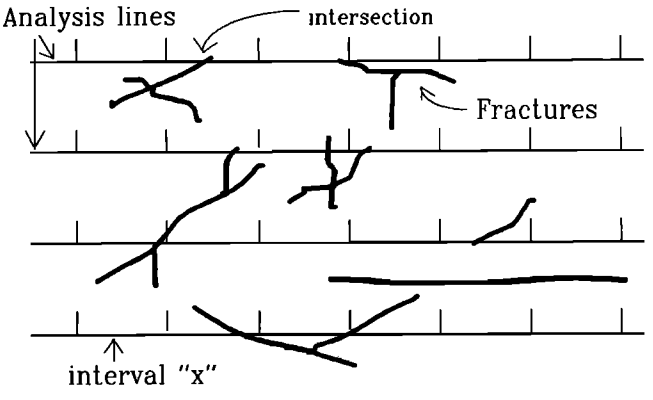

Fig.6. Representation of the Cantor's dust linear analysis of a fracture set. Dotted lines are the analysis lines, divided into segments of equal length; solid lines are the fractures.

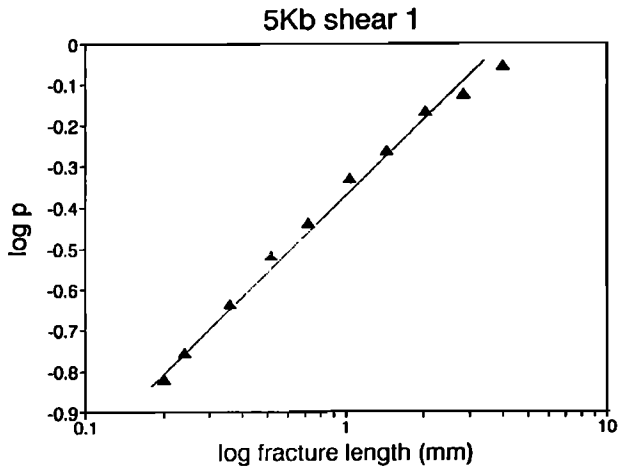

Fig.7. Example of fractal analysis (log measurement length x in mm against log proportion of units intersected by a fracture, given as p) for one data set from the 5 kbar confining pressure experiment.

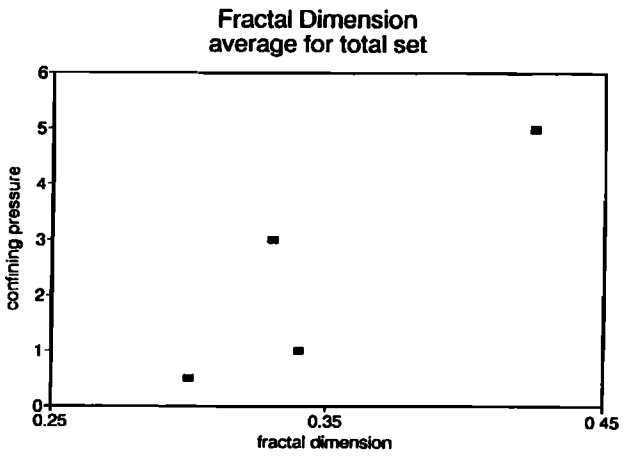

Fig.8. Average fractal dimension (D) of the total fracture pattern for different analysis orientation as a function of the confining pressures. Increase in D indicates a tendency to a greater regularity of distribution of the fractures.

tor's dust analysis consists on an estimation of the number of measurement units of x length on the analysis line which are intersected by a fracture trace. The proportion of measurement units intersected, (x_{int}) divided by the total of units on the analysis lines (x_{tot}), gives p which is the proportion of units affected. A plot of log x versus log p will give a linear relation in the case of a fractal relation. This is illustrated in Figure 7 for one set of data. Thus the plot of log(intersected units/total units) versus log(measurement unit length) gives a clear idea of the linearity which is necessary for a fractal relation (see *Velde et al.* [1990] for details). The fractal dimensions1 minus the slope of the relation above were determined for the entire fracture pattern as well as for those of the individual oriented sets. The individual fracture orientation setstension, decompression, and the two shear directions were measured in a direction perpendicular to the major orientation of the set. The full fracture set was analyzed in nine directions from horizontal (ie. perpendicular to the $\sigma 1$ direction) to parallel to this direction. This analysis assures that the different orientations are fully taken into account and it may have some importance concerning the origins of the confining linear method of Cantor's dust fractal analysis. Fractal pressures creating the fractures [*Velde et al.*, 1990]. The results given in Table 2 give the range of these nine values for the total fracture sets. Figures 8 and 9 show the evolution of the fractal values of the overall distribution and the difference between the highest and lowest value in each orientation set, i.e., shear, tension and decompresssion. The fractal analysis indicates that the fractal dimension of the total fracture set, and hence the regularity of occurrence of the fractures, increases with confining pressure. The individual fracture sets, according to orientation and hence origin, show a tendency to have similar fractal dimension for all orientationsand origins as confining pressure increases. This means that the spacial distribution of the fractures becomes more similar and more regular when confining pressure is increased. These results complement those of the statistical distribution of fracture lengths.

TABLE 2. Fractal Dimensions for the Fracture Sets According to Their Orientation

	Pressure, kbar			
	5	3	1	0.5
Total(0 - 90°)	0.40-0.45	0.36-0.30	0.38-0.30	0.28-0.32
Tension	0.24	0.29	0.38	0.43
Decompression	0.29	0.19	0.38	0.22
Shear 2	0.29	0.36	0.21	0.21
Shear 1	0.28	0.28	0.28	0.32

DISCUSSION AND CONCLUSIONS

In comparing the fractal dimension of the fracture sets of different origins (shear, tension, etc.) and their length distribution it is obvious that as confining pressure is increased the range of values for the fractures produced in a given experiment diminished. The fracture sets become more homogeneous and isometric, mode and average values of fracture lengths converge. Confining pressure therefore plays a role in the style of fractures generated during the experiments on the Barre Granite. In a very general way, the role of con-

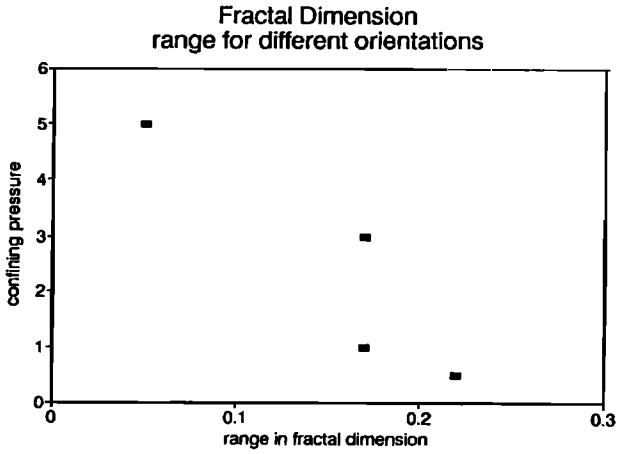

Fig.9. Difference between maximum and minimum values in D of the different orientations of fractures as a function of confining pressure. Decrease in range of D indicates a greater homogeneity in distribution between the different types of fracture. As confining pressure increases there is less difference between the distribution type (regularity) in each fracture orientation.

fining pressure is to increase the differential stress necessary to produce rock failure. If a high enough confining pressure is applied, over a sufficiently long period of time, the rock will show creep and plastic deformation. This is shown in the diagrams which summarize the experiments of *Peng and Johnson* [1972] given in Figure 1 by a change in shape of the specimen. The sample is shortened under higher confining pressure. The experiments can be taken, in a very general way, to represent the different stages in a continum of fracture and rock failure types between brittle and plastic behavior, even though all of the rocks failed in a brittle manner in the experiments. The above must be directly related to the observations made on the distributions of fractures of granitic rocks in geologic situations. Numerous studies have shown that the fractures in granites are fractal in nature ie. they are scale independent). This means that if one looks at a fault, it is in fact made up of many fractures, and a fracture is made up of many microfractures. This is not shocking, a priori. Studies on large fault systems [*Okubo and Aki*, 1987] such as the San Andreas fault in California have demonstrated that the fault is in fact a fault zone, whose component faults are distributed in a fractal nature. However, if one takes this proven observation to its logical conclusion, one must admit that a fracture (rupture in a rock) tends to engender or to be accompanied by other ruptures in its near field. This means that a fault is not a big, single, open and mobile plane of movement, at least in the granites, but it is in fact a zone of pseudo-plasticity where many ruptures occur on different scales. The fault is in fact a fault zone composed of a series of movement planes which themselves are composed of smaller units of rupture. If in fact the concept of fractality (events repeated on smaller scales inthe same manner) can be taken to the atomic scale, fault movement is totally plastic with each apparent rupture plane being in fact a microcosm of smaller rupture planes operating on smaller and smaller scales. This being true, fault planes observed on different scales are zones of plasticity especially in comparison to other, unruptured zones. Nevertheless, this concept must be confronted with the fact that fault plane single surfaces do exist, in the laboratory as well as in nature. At some point there is rupture on a single surface even though the rock may be multiply fractured adjacent to this surface. The change from fault breccia zone to that of "unfaulted rock" will be gradual. *Samis et al.* [1986] have shown that the dimensions of fault gouge also have fractal distributions, indicating that the process of fracture and total disaggregation of a rock are part of the same process. The observations in the areas outside of the central brecciated zone show fractal distributions, but those in the highly affected, central zone of the experiment will probably have different fractal values. We believe that there is a relation between the differences in the fractal dimension of fractures in a rock and the approach to a continuous, plastic style of deformation. This is seen in the qualitative descriptions of experiments of *Peng and Johnson* [1972] as well in the more numerical data presented here for similar experiments. The regularity of fracture length distribution and the fracture distribution in space indicate the degree of plasticity of the deformation in a rock deformed under rupture conditions. The irregularity of the fracture pattern will give an estimation of the violence of the rupture process. This should be related to seismic activity in larger-scale geologic events which engender earthquakes.

REFERENCES

Chernyshev, S. N. and W. R. Dearman, *Rock Fractures*, 777 pp, Butterworth Heinemann, London, 1991.

Davy, P., A. Sornette, and D. Sornette, Experimental discovery of scaling laws relating fractal dimension and length distribution exponent of fault systems, *Geophys. Res Lett., 19,* 361-364, 1992.

Goodman, R. E., *Introduction to Rock Mechanics,* 562 pp., John Wiley, New York, 1989.

Gudmundsson, A., Geometry, formation and development of tectonic fractures on the Reykjanes Peninsula, southwest Iceland, *Tectonophysics, 139,* 295-308, 1987.

Merceron, T., and B. Velde, Application of Cantor's dust method for fractal analysis of fractures in the Toyoha Mine, Hokkaido, Japan, *J. Geophys. Res., 96,* 16641 - 16650, 1991.

Moore, D., R. Summers, and J. D. Byrlee, Deformation of granite under triaxial stress friction tests, paper presented at International Conference on Mechanics of Jointed Faulted Rocks, Vienna, 1990.

Moore, D., R. Summers, and J. D. Byrlee, Faults, fractures and other deformation features produced during loading of granite in triaxial tests, *U.S. Geol. Surv. Open File Rep. 90.,* 1991.

Okubo, P.G., and K. Aki, Fractal geometry in the San Andreas Fault system, *J. Geophys. Res., 92,* 345-355, 1987.

Peng, S. and A. M. Johnson, Crack growth and faulting in cylindrical specimens of Chelmsford granite, *Int. J. Rock Mech. Min. Sci, 9,* 37-86, 1972.

Rock, N. M. S., *Numerical Geology,* 427 pp., Springer-Verlag, New York, 1988.

Samis, C. G., R. H. Osborne, J. L. Anderson, M. Banerdt, and P. White, Self-similar cataclasis in the formation of fault gouge, *Pure Appl. Geophys., 124,* 53-77, 1986.

Scholz, C. H., and P. A. Cowie, Determination of total strain from faulting using slip measurements, *Nature, 346,* 837-839, 1990.

Velde, B., J. Dubois, G. Touchard, and A. Badri, Fractal analysis of fractures in rocks: The Cantor's dust method, *Tectonophysics, 179,* 345-352, 1990.

Velde, B., J. Dubois, D. Moore, and G. Touchard, Fractal patterns of fractures in granites, *Earth Planet. Sci. Lett., 104,* 25-35, 1991.

Villemin, T. and C. Sunwoo, Self-similarity and logarithmic distribution of fault offsets and fault lengths in the Lorraine coal mines, *C. R. Acad. Sci., 305,* 1309-1312, 1987.

A. Badri, Laboratoire de Mécanique des Fluides, Université de Poitiers, Avenue Recteur Pineau, 86022, Poitiers, France.

B. Ledesert, Laboratoire des Altérations Hydrothermales, Université de Poitiers, Avenue Recteur Pineau, 86022, Poitiers, France.

D. Moore, U.S. Geological Survey, 345 Middlefield Road, Menlo Park, CA 94025.

B. Velde, Département de Géologie, UR 1316, Ecole Normale Supérieure, 24 rue Lhomond, 75235 Paris, France.

(Received April 21, 1992;
revised September 14, 1992;
accepted October 23, 1992.)